Influence of the cathode size on the CCD

Dong-Hyuk Park, Hae-Kyun Park and Bum-Jin Chung*
Department of Nuclear Engineering, Kyung Hee University
#1732 Deogyeong-daero, Giheung-gu, Yongin-si, Gyeonggi-do, 17104, Korea
**Corresponding author: bjchung@khu.ac.kr*

1. Introduction

Boiling heat transfer is widely used in many industries, since it can achieve a large heat transfer rate than single phase heat transfer. However, when the heat flux exceeds a certain a level, a vapor film is formed on the heating surface, resulting in an abrupt increase in the surface temperature, called the critical heat flux (CHF) [1]. Especially in the nuclear power plant, it is important to measure the CHF as the limiting condition. Meanwhile, the CHF experiment is difficult to perform due to the extreme experimental condition which result in failure of experimental apparatus and measurement devices. In order to avoid this experimental difficulty, an alternative experimental method is being explored by the authors' research group [2-9].

In an electrochemical hydrogen evolving system such as water electrolysis, the cell potential increases as the current density increases due to the increased hydrogen generation rate. When the current density reaches a certain critical limit, hydrogen film is formed at the cathode surface and then the cell potential increases abruptly. This phenomenon is known as the critical current density (CCD) [10]. Based on the analogous relation, the heat flux and the temperature in the boiling system correspond to the current density and the cell potential in the hydrogen evolving system [6,7].

The previous studies revealed that the gas film formation phenomenon on the cathode surface is governed by hydrodynamic parameters, similar to that of the boiling system [6,7]. Thus, we postulated that there is a further analogous relationship between the CHF and the CCD. The CCDs were measured according to the cathode size, which generates hydrogen gas together with the visualization of bubble behaviors using high-speed camera.

2. Existing studies

2.1 Analogous relation between CHF and CCD

The authors' previous work [6,7] reported that the dry spot model and macrolayer dryout model, which are the CHF models can be applied to the CCD phenomenon. And Han et al. [8] and Park et al. [9] confirmed analogous influences of mass flux, inclination and inlet void fraction on the CCD to the CHF. This implies that there is a further analogous relation between the CHF and the CCD in terms of the hydrodynamics.

2.2 Influnece of heater size on CHF

Several CHF studies [11-15] commonly reported that the CHF decreases as the heater size increases due to the enhanced rewetting resistance from bulk fluid to the heater center. Rainey and You [11] insisted that a portion of the rewetting fluid which is supplied from the heater side became larger than that from the above as the heater size decreased.

3. Experimental setup

Figure 1 shows the experimental apparatus and electric circuit. We used 1.5 M aqueous solution of sulfuric acid (H_2SO_4) at atmospheric condition and room temperature (294 K). The copper cathode was used, which generates hydrogen bubbles and is designed as an upward-facing disk plate. The cathode surface was polished by using 2000 grit emery paper to maintain the bare surface condition. The size of cathode (L) is varied from 5 mm to 30 mm as shown in Table 1. Power supply was used to control the cell potential and the current density. The electric data was recorded using a data acquisition (DAQ) system. The high-speed camera was used to record the bubble behaviors at each cathode size.

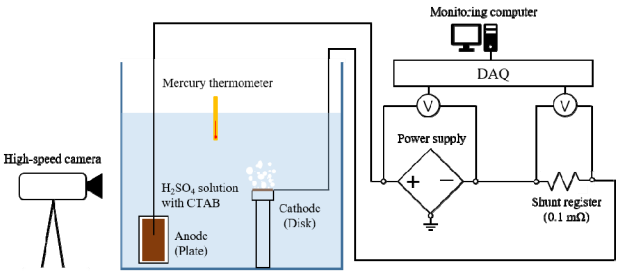

Fig. 1. Experimental apparatus and test section.

Table 1. Variation of cathode size.

Configuration of cathode	Cathode size, L (mm)
Upward-facing disk	5 10 15 20 30

4. Results and discussion

4.1 Hydrogen bubble behaviors according to the E-I curve

Figure 2 and 3 show the bubble behaviors according to *E-I* curves. Similar trends of *E-I* curves were measured regardless of the *L*. As the cell potential increased, the hydrogen gas generation became more vigorous with increased current density as shown in the points (a-d) of the Figs. 2 and 3. When the cell potential reaches a certain level the current density is limited due to partial hydrogen film as shown in the point (e). However, different bubble behaviors were observed after the CCD point according to the *L*. In case of the small *L*, Fig. 2(f), a stable hydrogen film was formed on the surface, while somewhat unstable hydrogen film was formed in Fig. 3(f). It is due to the increased *L*, which cannot be covered by a single hydrogen film. Thus, the current density did not drop drastically in case of the *L* = 30 mm as did in the *L* = 5 mm case.

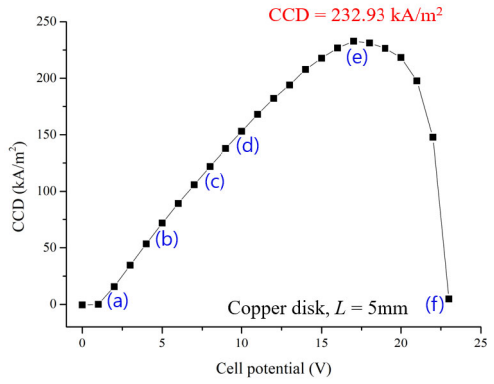

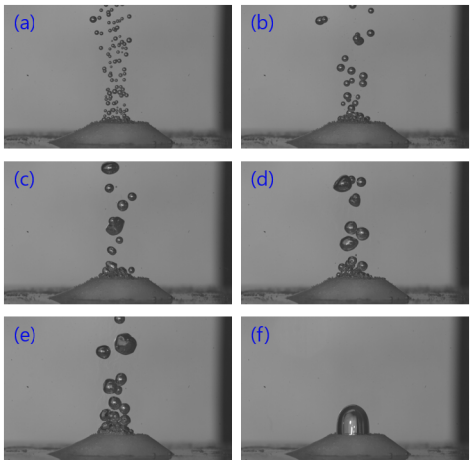

Fig. 2. *E-I* curve and hydrogen bubble behaviors; *L* = 5 mm.

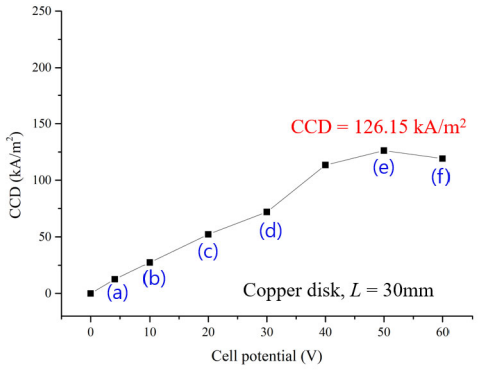

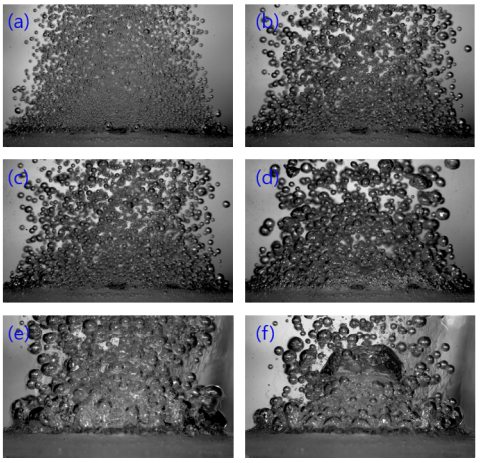

Fig. 3. *E-I* curve and hydrogen bubble behaviors; *L* = 30 mm.

4.2 Comparison of bubble behaviors between CHF and CCD according to the surface

Figure 4 shows bubble behaviors of the boiling and hydrogen evolving systems. The white lines denote the location of the surface. Smaller bubbles are observed in the hydrogen evolving system (right column) than that of the boiling system (left column). This is due to the nucleation characteristics of the hydrogen evolving system: Small bubble departure diameter and high nucleation site density compared to the typical water boiling systems [4]. Thus, the hydrogen generation rate at the CCD is much smaller than the water boiling system, which results in the different bubble behaviors as shown in the Fig. 4. However, at the 30 mm case in the hydrogen evolving system, hydrogen mushroom is observed over the surface, similar to the boiling system. The increased hydrogen generation due to the increased *L* facilitates the formation of the hydrogen mushroom.

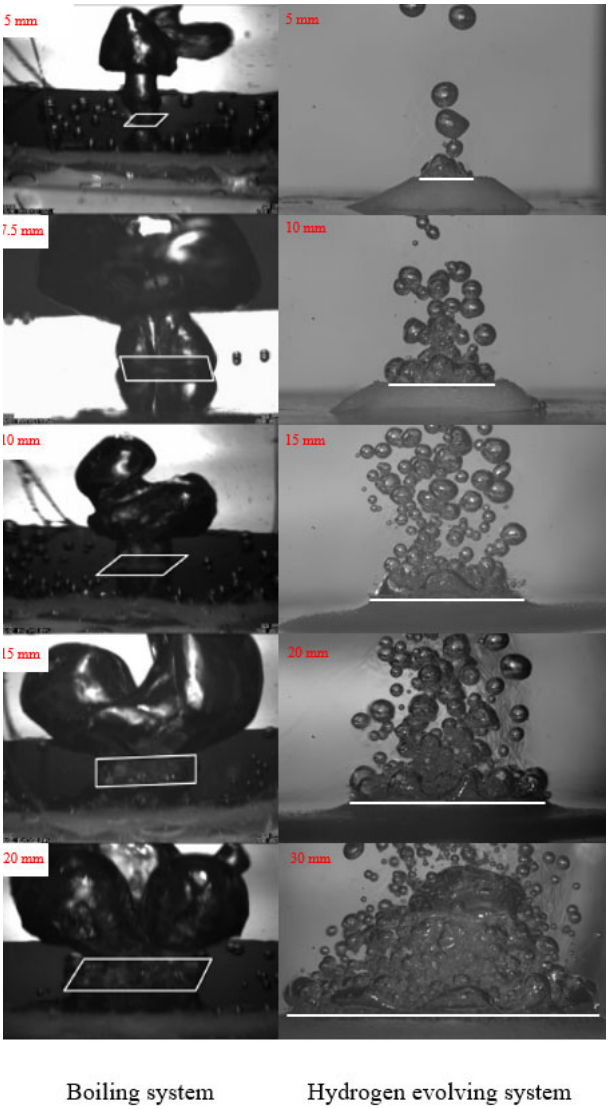

Fig. 4. Comparison of bubble behavior just before the CHF and CCD according to the surface size; left column denotes boiling system [14] and right column denotes present result.

Figure 5 shows formation process of the hydrogen mushroom in case of L = 30 mm. Vigorous nucleate bubbles at 0 ms started to coalescence into a hydrogen mushroom (20 to 40 ms). Subsequently, the hydrogen mushroom is finally departed from the cathode surface (60 ms). This phenomenon is periodically occurred.

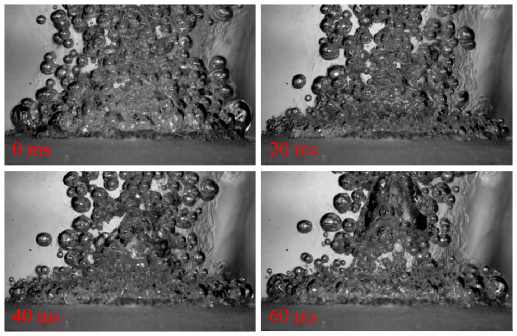

Fig. 5. Formation of hydrogen mushroom.

4.3 Variation of CCD according to the surface size

Figure 6 shows measured CCD according to the L. The present results are compared to the previous CHF studies [12-14]. The CCD decreased with increased L. The same tendency appeared in CHF results. This can be explained by the increased rewetting resistance with the increased L, same with CHF. When the current density is increased, the generation rate of hydrogen gas at the cathode increased as shown in the Fig. 2 and 3. The increased hydrogen gas generation near the CCD disturbs the inflow of bulk liquid from the above, thus the rewetting phenomenon is mainly caused by side flow. Hence, the increased L increases the fluid path length to reach the center of the cathode; enhanced rewetting resistance. This phenomenon results in the decreased CCD with increased L. Despite the different bubble behavior between the boiling and hydrogen evolving systems, it is revealed that the two systems share the influence of L, which shows analogy in terms of hydrodynamics.

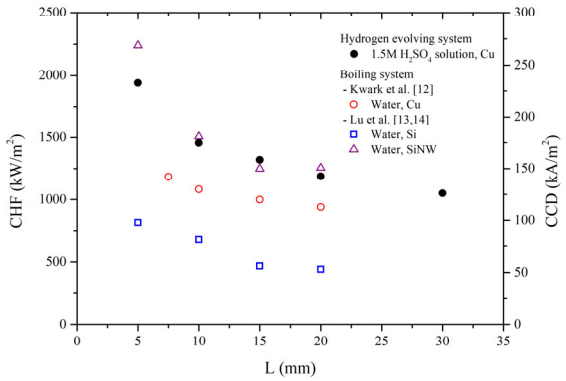

Fig. 6. The influence of L on CCD and CHF [12-14].

5. Conclusions

The CCDs were measured varying the cathode surface size to confirm an analogous relation between the CHF and the CCD.

Photographic analyses showed the increased hydrogen generation rate with the current density increased. Similar to the CHF phenomenon, hydrogen film is formed at the cathode surface at a certain high current density, CCD.

The CCD decreased as the cathode size increased, similar to the CHF. Due to the nucleation characteristics of the hydrogen evolving system, smaller hydrogen bubbles are observed than the water boiling system. Despite the different bubble size, it seems that the CCD is subjected by the enhanced rewetting resistance as the cathode size increased, similar to the CHF when the heater size is increased.

This work proves the additional analogous relation between the CHF and the CCD in the aspect of hydrodynamics.

ACKNOWLEDEGEMENT

This study was sponsored by the Ministry of Science and ICT (MSIT) and was supported by nuclear Research & Development program grant funded by the National Research Foundation (NRF) (Grant codes 2020M2D2A1A02065563)

REFERENCES

[1] G. Liang and I. Mudawar, Pool boiling critical heat flux (CHF) – Part 1: Review of mechanisms, models, and correlations, International Journal of Heat and Mass Transfer, Vol.117, pp.1352-1367, 2018.
[2] S. M. Ohk, H. K. Park, B. J. Chung, CHF experiments on the influence of inclination and gap size, International Journal of Heat and Mass Transfer, Vol. 132, pp. 929-938, 2019.
[3] H. K. Park and B. J. Chung, Simulation of critical heat flux phenomenon using a non-heating hydrogen evolving system, Frontiers in Energy Research, Vol. 7, 139, 2019.
[4] H. K. Park and B. J. Chung, Comparison of bubble parameters between boiling and hydrogen evolving systems, Experimental Thermal and Fluid Science, Vol. 122, 110316, 2021.
[5] H. K. Park and B. J. Chung, Comparative analysis of bubble behavior between boiling and hydrogen evolving system at horizontal cylinders, Heat and Mass Transfer, 2021, (online published).
[6] H. K. Park and B. J. Chung, Application of macrolayer dryout model for the critical current density of water electrolysis, International Communications in Heat and Mass Transfer, Vol. 130, 105759, 2022.
[7] H. K. Park and B. J. Chung, Estimation of critical number of hydrogen bubbles for critical current density using the dry spot model, Chemical Engineering Science, Vol 249, 117344, 2022.
[8] J. W. Han, D. Y. Lee, H. K. Park, B. J. Chung, Experimental investigation on the flow CCD by analogically utilizing the CHF correlation, International Journal of Heat and Mass Transfer, Vol. 183,122242, 2022.
[9] H. K. Park, J. W. Han, B. J. Chung, Influence of hydrodynamic parameters on the critical current density at water electrolysis: Mass flux, channel inclination and inlet void fraction, International Journal of Hydrogen Energy, Vol. 47, pp. 7535-7546, 2022.
[10] H. Vogt, Heat transfer in boiling and mass transfer in gas evolution at electrodes – The analogy and its limits, International Journal of Heat and Mass Transfer, Vol 59, pp. 191-197, 2013.
[11] K. N. Rainey and S.M. You, Effects of heater size and orientation on pool boiling heat transfer from microporous coated surfaces, International Journal of Heat and Mass Transfer, Vol. 44, pp. 2589-2599, 2001.
[12] S. M. Kwark, M. Amaya, R. Kumar. G. Moreno, S.M. You, Effects of pressure, orientation, and heater size on pool boiling of water with nanocoated heaters, International Journal of Heat and Mass Transfer, Vol. 53, pp. 5199-5208, 2010.
[13] M. C. Lu, R. Chen, V. Srinivasan, V. P. Carey A. Majumdar, Critical heat flux of pool boiling on Si nanowire array-coated surfaces, International Journal of Heat and Mass Transfer, Vol. 54, pp. 5359-5367, 2011.
[14] M. C. Lu, C. H. Huang, C. T. Huang, Y. C. Chen, A modified hydrodynamic model for pool boiling CHF considering the effects of heater size and nucleation site density, International Journal of Thermal Sciences, Vol. 91, pp. 133-141, 2015.
[15] M. He, Y. Lee, Revisiting heater size sensitive pool boiling critical heat flux using neural network modeling: Heater length of the half of the Rayleigh-Taylor Instability Wavelength maximizes CHF, Thermal Science and Engineering Progress, Vol. 14, 100421, 2019.